J|A|C|S
ARTICLES
Published on Web 03/02/2006

3,3′-Bis(trisarylsilyl)-Substituted Binaphtholate Rare Earth Metal Catalysts for Asymmetric Hydroamination

Denis V. Gribkov, Kai C. Hultzsch,* and Frank Hampel

Contribution from the Institut für Organische Chemie, Friedrich-Alexander Universität Erlangen-Nürnberg, Henkestrasse 42, D-91054 Erlangen, Germany

Received December 6, 2005; E-mail: hultzsch@chemie.uni-erlangen.de

Abstract: Chiral 3,3′-bis(trisarylsilyl)-substituted binaphtholate rare earth metal complexes (*R*)-[Ln{Binol-$SiAr_3$}(*o*-$C_6H_4CH_2NMe_2$)(Me_2NCH_2Ph)] (Ln = Sc, Lu, Y; Binol-$SiAr_3$ = 3,3′-bis(trisarylsilyl)-2,2′-dihydroxy-1,1′-binaphthyl; Ar = Ph (**2-Ln**), 3,5-xylyl (**3-Ln**)) and (*R*)-[La{Binol-Si(3,5-xylyl)$_3$}{E($SiMe_3$)$_2$}(THF_2] (E = CH (**4a**), N (**4b**)) are accessible via facile arene, alkane, and amine elimination. They are efficient catalysts for the asymmetric hydroamination/cyclization of aminoalkenes, giving TOF of up to 840 h^{-1} at 25 °C for 2,2-diphenyl-pent-4-enylamine (**5c**) using (*R*)-**2-Y**. Enantioselectivities of up to 95% ee were achieved in the cyclization of **5c** with (*R*)-**2-Sc**. The reactions show apparently zero-order rate dependence on substrate concentration and first-order rate dependence on catalyst concentration, but rates depend on total amine concentrations. Activation parameters for the cyclization of pent-4-enylamine using (*R*)-**2-Y** ($\Delta H(S)^{\ddagger} = 57.4(0.8)$ kJ mol^{-1} and $\Delta S(S)^{\ddagger} = -102(3)$ J K^{-1} mol^{-1}; $\Delta H(R)^{\ddagger} = 61.5(0.7)$ kJ mol^{-1} and $\Delta S(R)^{\ddagger} = -103(3)$ J K^{-1} mol^{-1}) indicate a highly organized transition state. The binaphtholate catalysts were also applied to the kinetic resolution of chiral α-substituted aminoalkenes with resolution factors *f* of up to 19. The 2,5-disubstituted aminopentenes were formed in 7:1 to ≥50:1 *trans* diastereoselectivity, depending on the size of the α-substituent of the aminoalkene. Rate studies with (*S*)-1-phenyl-pent-4-enylamine ((*S*)-**15e**) gave the activation parameters for the matching ($\Delta H^{\ddagger} = 52.2(2.8)$ kJ mol^{-1}, $\Delta S^{\ddagger} = -127(8)$ J K^{-1} mol^{-1} using (*S*)-**2-Y**) and mismatching ($\Delta H^{\ddagger} = 57.7(1.3)$ kJ mol^{-1}, $\Delta S^{\ddagger} = -126(4)$ J K^{-1} mol^{-1} using (*R*)-**2-Y**) substrate/catalyst combination. The absolute configuration of the Mosher amide of (2*S*)-2-methyl-4,4-diphenyl-pyrrolidine and (2*R*)-methyl-(5*S*)-phenyl-pyrrolidinium chloride, prepared from (*S*)-**15e**, were determined by crystallographic analysis. Catalyst (*R*)-**4a** showed activity in the *anti*-Markovnikov addition of *n*-propylamine to styrene.

Introduction

The importance of nitrogen-containing compounds in biological systems and industrially relevant basic and fine chemicals has sparked significant research efforts to develop efficient synthetic protocols.[1] One of the simplest approaches, the hydroamination, has found significant attention only in recent years with the development of more efficient transition metal based catalyst systems.[2] The addition of amine N−H functionalities to unsaturated carbon−carbon bonds, either in an *inter*molecular (eq 1) or *intra*molecular (eq 2) fashion, generates amines in a waste-free, highly atom-economical manner starting from simple and inexpensive precursors.

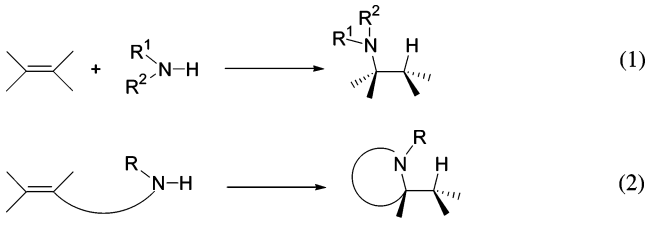

Transition metal based hydroamination catalysts have the significant advantage that they permit facile tuning of catalytic properties via adjustment of sterical and electronic features of the ligand framework, thereby controlling the stereo- and regiochemistry of the hydroamination product. In particular the generation of new stereogenic centers constitutes an attractive application of the hydroamination process, but the development of chiral catalysts for the asymmetric hydroamination of alkenes (AHA) has remained challenging.[3]

(1) Malpass, J. R. In *Comprehensive Organic Chemistry*; Barton, D., Ollis, W. D., Eds.; Pergamon Press: Oxford, 1979; Vol. 2, p 1.

(2) For general and comprehensive reviews on this topic see: (a) Taube, R. In *Applied Homogeneous Catalysis*; Cornils, B., Herrmann, W. A., Eds.; VCH: Weinheim, 1996; Vol. 1, p 507. (b) Müller, T. E.; Beller, M. *Chem. Rev.* **1998**, *98*, 675. (c) Müller, T. E.; Beller, M. In *Transition Metals for Organic Synthesis*; Beller, M., Bolm, C., Eds.; Wiley-VCH: Weinheim, 1998; Vol. 2, p 316. (d) Brunet, J. J.; Neibecker, D. In *Catalytic Heterofunctionalization from Hydroamination to Hydrozirconation*; Togni, A., Grützmacher, H., Eds.; Wiley-VCH: Weinheim, 2001; p 91. (e) Nobis, M.; Driessen-Hölscher, B. *Angew. Chem., Int. Ed.* **2001**, *40*, 3983. (f) Seayad, J.; Tillack, A.; Hartung, C. G.; Beller, M. *Adv. Synth. Catal.* **2002**, *344*, 795. (g) Beller, M.; Breindl, C.; Eichberger, M.; Hartung, C. G.; Seayad, J.; Thiel, O. R.; Tillack, A.; Trauthwein, H. *Synlett* **2002**, 1579. (h) Hartwig, J. F. *Pure Appl. Chem.* **2004**, *76*, 507. (i) Pohlki, F.; Doye, S. *Chem. Soc. Rev.* **2003**, *32*, 104. (j) Bytschkov, I.; Doye, S. *Eur. J. Org. Chem.* **2003**, 935. (k) Doye, S. *Synlett* **2004**, 1653. (l) Hong, S.; Marks, T. J. *Acc. Chem. Res.* **2004**, *37*, 673. (m) Odom, A. L. *Dalton Trans.* **2005**, 225.

(3) (a) Roesky, P. W.; Müller, T. E. *Angew. Chem., Int. Ed.* **2003**, *42*, 2708. (b) Hultzsch, K. C. *Adv. Synth. Catal.* **2005**, *347*, 367. (c) Hultzsch, K. C. *Org. Biomol. Chem.* **2005**, *3*, 1819. (d) Hultzsch, K. C.; Gribkov, D. V.; Hampel, F. *J. Organomet. Chem.* **2005**, *690*, 4441.

10.1021/ja058287t CCC: $33.50

Catalyst systems based on alkali and alkaline earth metals,[2a−d,f,4] as well as early (groups 3−5, lanthanides and actinides)[2i−m,5,6] and late (groups 8−10)[2g,h,7] transition metals have been developed. Unfortunately, many of these systems can be applied only to a limited set of substrates. Commonly, only activated alkenes [e.g. alkenes with electron-withdrawing groups attached, vinyl arenes, 1,3-dienes, or ring-strained alkenes], alkynes, or certain types of amines [e.g., anilines] can be applied. Rare earth metals based catalyst systems are reactive toward simple alkene substrates, predominantely in intramolecular reactions.[2l,8−10]

The first chiral rare earth metal based hydroamination catalysts were reported by Marks and co-workers in 1992.[9a,b,11] Although enantioselectivities of up to 74% ee were achieved, the application of these C_1-symmetric chiral *ansa*-lanthanocenes was limited due to a facile epimerization process via reversible protolytic cleavage of the metal cyclopentadienyl bond under the reaction conditions of catalytic hydroamination.[9b−e] The configuration of the hydroamination products was independent of diastereomeric purity of the lanthanocene precatalysts, requiring a catalyst redesign if the opposite enantiomer of the hydroamination product is desired.[9b]

We therefore decided to develop hydroamination catalyst systems based on non-cyclopentadienyl ligand sets,[12] which should have comparable catalytic activity to the lanthanocene systems but should retain their configurational integrity under the reaction conditions of catalytic hydroamination. Furthermore, chiral non-cyclopentadienyl ligand sets are usually easily accessible and can be readily modified.[13] Increased interest in this area in recent years has surfaced in several reports on non-metallocene rare earth metal based catalyst systems[14] for enantioselective[3b−d,15−17] hydroamination.

In our initial studies on biphenolate and binaphtholate rare earth metal hydroamination catalysts[16] we realized that sterically demanding substituents in 3 and 3′ positions of the diolate ligand are an indispensable requirement for a monomeric catalyst structure and effective asymmetric induction. We therefore anticipated that an increase in steric bulk of these substituents would increase enantioselectivity. In this paper we report the synthesis of 3,3′-bis(trisarylsilyl)-substituted binaphtholate rare earth metal complexes and their application as hydroamination catalysts.[17] Schaverien reported the synthesis of similar binaphtholate alkyllanthanum complexes more than a decade ago,[18] but their catalytic potential has remained unexplored to date.

(4) Crimmin, M. R.; Casely, I. J.; Hill, M. S. *J. Am. Chem. Soc.* **2005**, *127*, 2042.

(5) For some examples using actinide-based catalysts, see: (a) Straub, T.; Haskel, A.; Neyroud, T. G.; Kapon, M.; Botoshansky, M.; Eisen, M. S. *Organometallics* **2001**, *20*, 5017. (b) Wang, J.; Dash, A. K.; Kapon, M.; Berthet, J.-C.; Ephritikhine, M.; Eisen, M. S. *Chem. Eur. J.* **2002**, *8*, 5384. (c) Stubbert, B. D.; Stern, C. L.; Marks, T. J. *Organometallics* **2003**, *22*, 4836.

(6) For some recent examples using group 4- and group 5-based catalyst systems, see: (a) Ackermann, L.; Bergman, R. G.; Loy, R. N. *J. Am. Chem. Soc.* **2003**, *125*, 11956. (b) Knight, P. D.; Munslow, I.; O'Shaughnessy, P. N.; Scott, P. *Chem. Commun.* **2004**, 894. (c) Ackermann, L.; Kaspar, L. T.; Gschrei, C. J. *Org. Lett.* **2004**, *6*, 2515. (d) Anderson, L. L.; Arnold, J.; Bergman, R. G. *Org. Lett.* **2004**, *6*, 2519. (e) Ramanathan, B.; Keith, A. J.; Armstrong, D.; Odom, A. L. *Org. Lett.* **2004**, *6*, 2957. (f) Heutling, A.; Pohlki, F.; Doye, S. *Chem. Eur. J.* **2004**, *10*, 3059. (g) Pohlki, F.; Bytschkov, I.; Siebeneicher, H.; Heutling, A.; König, W. A.; Doye, S. *Eur. J. Org. Chem.* **2004**, 1967. (h) Lorber, C.; Choukroun, R.; Vendler, L. *Organometallics* **2004**, *23*, 1845. (i) Hoover, J. M.; Petersen, J. R.; Pikul, J. H.; Johnson, A. R. *Organometallics* **2004**, *23*, 4614. (j) Gribkov, D. V.; Hultzsch, K. C. *Angew. Chem., Int. Ed.* **2004**, *44*, 5542. (k) Bexrud, J. A.; Beard, J. D.; Leitch, D. C.; Schafer, L. L. *Org. Lett.* **2005**, *7*, 1959. (l) Kim, H.; Lee, P. H.; Livinghouse, T. *Chem. Commun.* **2005**, 5205. (m) Marcseková, K.; Wegener, B.; Doye, S. *Eur. J. Org. Chem.* **2005**, 4843. (n) Tillack, A.; Khedkar, V.; Jiao, H.; Beller, M. *Eur. J. Org. Chem.* **2005**, 5001.

(7) For some recent examples using late transition metal catalyst systems, see: (a) Kawatsura, M.; Hartwig, J. F. *J. Am. Chem. Soc.* **2000**, *122*, 9546. (b) Löber, O.; Kawatsura, M.; Hartwig, J. F. *J. Am. Chem. Soc.* **2001**, *123*, 4366. (c) Lutete, L. M.; Kadota, I.; Yamamoto, Y. *J. Am. Chem. Soc.* **2004**, *126*, 1622. (d) Utsunomiya, M.; Kuwano, R.; Kawatsura, M.; Hartwig, J. F. *J. Am. Chem. Soc.* **2003**, *125*, 5608. (e) Utsunomiya, M.; Hartwig, J. F. *J. Am. Chem. Soc.* **2004**, *126*, 2702. (f) Vo, L. K.; Singleton, D. A. *Org. Lett.* **2004**, *6*, 2469. (g) Tillack, A.; Khedkar, V.; Beller, M. *Tetrahedron Lett.* **2004**, *45*, 8875. (h) Bender, C. F.; Widenhoefer, R. A. *J. Am. Chem.* Soc. **2005**, *127*, 1070. (i) Takaya, J.; Hartwig, J. F. *J. Am. Chem. Soc.* **2005**, *127*, 5756. (j) Yi, C. S.; Yun, S. Y.; Guzei, I. A. *J. Am. Chem. Soc.* **2005**, *127*, 5782. (k) Brunet, J.-J.; Chu, N. C.; Diallo, O. *Organometallics* **2005**, *24*, 3104. (l) Zulys, A.; Dochnahl, M.; Hollmann, D.; Löhnwitz, K.; Herrmann, J.-S.; Roesky, P. W.; Blechert, S. *Angew. Chem., Int. Ed.* **2005**, *44*, 7794.

(8) For hydroamination catalyzed by cyclopentadienyl rare earth metal complexes see: (a) Gagné, M. R.; Marks, T. J. *J. Am. Chem. Soc.* **1989**, *111*, 4108. (b) Gagné, M. R.; Stern, C. L.; Marks, T. J. *J. Am. Chem. Soc.* **1992**, *114*, 275. (c) Li, Y.; Marks, T. J. *J. Am. Chem. Soc.* **1996**, *118*, 9295. (d) Li, Y.; Marks, T. J. *J. Am. Chem.* Soc. **1998**, *120*, 1757. (e) Gilbert, A. T.; Davis, B. L.; Emge, T. J.; Broene, R. D. *Organometallics* **1999**, *18*, 2125. (f) Arredondo, V. M.; Tian, S.; McDonald, F. E.; Marks, T. J. *J. Am. Chem. Soc.* **1999**, *121*, 3633. (g) Molander, G. A.; Dowdy, E. D. *J. Org. Chem.* **1999**, *64*, 6515. (h) Arredondo, V. M.; McDonald, F. E.; Marks, T. J. *Organometallics* **1999**, *18*, 1949. (i) Molander, G. A.; Dowdy, E. D.; Pack, S. K. *J. Org. Chem.* **2001**, *66*, 4344. (j) Molander, G.; Pack, S. K. *Tetrahedron* **2003**, *59*, 10581. (k) Molander, G. A.; Pack, S. K. *J. Org. Chem.* **2003**, *68*, 9214.

(9) For asymmetric hydroamination catalyzed by cyclopentadienyl rare earth metal complexes see: (a) Gagné, M. R.; Brard, L.; Conticello, V. P.; Giardello, M. A.; Marks, T. J.; Stern, C. L. *Organometallics* **1992**, *11*, 2003. (b) Giardello, M. A.; Conticello, V. P.; Brard, L.; Gagné, M. R.; Marks, T. J. *J. Am. Chem. Soc.* **1994**, *116*, 10241. (c) Douglass, M. R.; Ogasawara, M.; Hong, S.; Metz, M. V.; Marks, T. J. *Organometallics* **2002**, *21*, 283. (d) Hong, S.; Kawaoka, A. M.; Marks, T. J. *J. Am. Chem. Soc.* **2003**, *125*, 15878. (e) Ryu, J.-S.; Marks, T. J.; McDonald, F. E. *J. Org. Chem.* **2004**, *69*, 1038.

(10) Most investigations utilizing rare earth metal catalysts have focused on *intramolecular* hydroamination reactions, whereas the number of reports on *intermolecular* hydroamination are limited, see: (a) Li, Y.; Marks, T. J. *Organometallics* **1996**, *15*, 3770. (b) Ryu, J.-S.; Li, G. Y.; Marks, T. J. *J. Am. Chem. Soc.* **2003**, *125*, 12584.

(11) For reviews on the application of chiral rare earth metal catalysts in organic synthesis, see: (a) Mikami, K.; Terada, M.; Matsuzawa, H. *Angew. Chem., Int. Ed.* **2002**, *41*, 3554. (b) Aspinall, H. C. *Chem. Rev.* **2002**, *102*, 1807. (c) Shibasaki, M.; Yoshikawa, N. *Chem. Rev.* **2002**, *102*, 2187. (d) Kobayashi, S.; Sugiura, M.; Kitagawa, H.; Lam, W. W.-L. *Chem. Rev.* **2002**, *102*, 2227.

(12) For general reviews on the chemistry of cyclopentadienyl-free rare earth metal complexes see: (a) Edelmann, F. T. *Angew. Chem., Int. Ed. Engl.* **1995**, *34*, 2466. (b) Edelmann, F. T.; Freckmann, D. M. M.; Schumann, H. *Chem. Rev.* **2002**, *102*, 1851. (c) Piers, W. E.; Emslie, D. J. H. *Coord. Chem. Rev.* **2002**, *233−234*, 131.

(13) Even simple modifications to the ligand structure of cyclopentadienyl ligands can require tedious multistep procedures; see for example: (a) Halterman, R. L. *Chem. Rev.* **1992**, *92*, 2, 965. (b) Halterman R. L. In *Metallocenes*; Togni, A., Halterman, R. L., Eds.; Wiley-VCH: Weinheim, 1998; Vol. 1, p 455.

(14) For achiral non-metallocene rare earth metal based hydroamination catalysts, see: (a) Bürgstein, M. R.; Berberich, H.; Roesky, P. W. *Organometallics* **1998**, *17*, 1452. (b) Bürgstein, M. R.; Berberich, H.; Roesky, P. W. *Chem. Eur. J.* **2001**, *7*, 3078. (c) Kim, Y. K.; Livinghouse, T.; Bercaw, J. E. *Tetrahedron Lett.* **2001**, *42*, 2933. (d) Kim, Y. K.; Livinghouse, T. *Angew. Chem., Int. Ed.* **2002**, *41*, 3645. (e) Kim, Y. K.; Livinghouse, T.; Horino, Y. *J. Am. Chem. Soc.* **2003**, *125*, 9560. (f) Lauterwasser, F.; Hayes, P. G.; Bräse, S.; Piers, W. E.; Schafer, L. L. *Organometallics* **2004**, *23*, 2234. (g) Hultzsch, K. C.; Hampel, F.; Wagner, T. *Organometallics* **2004**, *23*, 2601. (h) Panda, T. K.; Zulys, A.; Gamer, M. T.; Roesky, P. W. *Organometallics* **2005**, *24*, 2197. (i) Kim, J. Y.; Livinghouse, T. *Org. Lett.* **2005**, *7*, 4391. (j) Bambirra, S.; Tsurugi, H.; van Leusen, D.; Hessen, B. *Dalton Trans* **2006**, 1157.

(15) (a) O'Shaughnessy, P. N.; Knight, P. D.; Morton, C.; Gillespie, K. M.; Scott, P. *Chem. Commun.* **2003**, 1770. (b) O'Shaughnessy, P. N.; Scott, P. *Tetrahedron Asymmetry* **2003**, *14*, 1979. (c) Hong, S.; Tian, S.; Metz, M. V.; Marks, T. J. *J. Am. Chem. Soc.* **2003**, *125*, 14768. (d) Collin, J.; Daran, J.-D.; Schulz, E.; Trifonov, A. *Chem. Commun.* **2003**, 3048. (e) O'Shaughnessy, P. N.; Gillespie, K. M.; Knight, P. D.; Munslow, I.; Scott, P. *Dalton Trans.* **2004**, 2251. (f) Kim, J. Y.; Livinghouse, T. *Org. Lett.* **2005**, *7*, 1737. (g) Collin, J.; Daran, J.-D.; Jacquet, O.; Schulz, E.; Trifonov, A. *Chem. Eur. J.* **2005**, *11*, 3455.

(16) (a) Gribkov, D. V.; Hultzsch, K. C.; Hampel, F. *Chem. Eur. J.* **2003**, *9*, 4796. (b) Gribkov, D. V.; Hampel, F.; Hultzsch, K. C. *Eur. J. Inorg. Chem.* **2004**, 4091.

(17) A preliminary account of the results presented herein has been communicated, see: Gribkov, D. V.; Hultzsch, K. C. *Chem. Commun.* **2004**, 730.

(18) Schaverien, C. J.; Meijboom, N.; Orpen, A. G. *J. Chem. Soc., Chem. Commun.* **1992**, 124.

Scheme 1

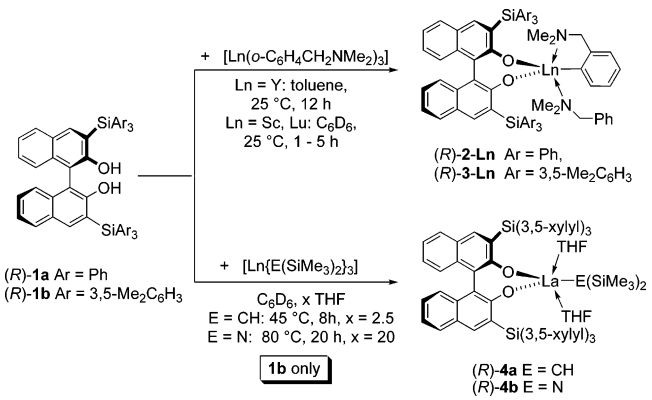

Results

Synthesis of Binaphtholate Complexes. Binaphtholate rare earth metal complexes of the smaller rare earth elements, scandium, yttrium, and lutetium, were prepared via arene elimination from the readily available homoleptic tris(aryl) complexes [Ln(*o*-$C_6H_4CH_2NMe_2)_3$] (Ln = Sc, Y, Lu)[19] using the tris(aryl)silyl binaphthols[20] (*R*)-**1a** and (*R*)-**1b** (Scheme 1). Complexes (*R*)-**2-Ln** and (*R*)-**3-Ln** retained one equivalent of *N*,*N*-dimethylbenzylamine coordinated to the metal center (by NMR spectroscopy). Although the reactions proceeded cleanly by NMR spectroscopy (see Supporting Information), removal of traces of free *N*,*N*-dimethylbenzylamine proved to be difficult in preparative-scale reactions.[21] Therefore, the catalysts were often prepared in situ or stored as a frozen stock solution in C_6D_6 at −35 °C. Exchange between coordinated and free benzylamine was slow on the NMR time scale. However, the coordinated *N*,*N*-dimethylbenzylamine could be readily displaced by harder donors, such as THF.[22]

Tris(3,5-xylyl)silyl-substituted binaphtholate complexes of the larger lanthanum metal were accessible either from the tris(alkyl) complex [La{$CH(SiMe_3)_2$}$_3$][23a] at room temperature or the tris(amido) complex [La{$N(SiMe_3)_2$}$_3$][23b] at 80 °C (Scheme 1).[24] While (*R*)-**4a** was cleanly formed in the presence of 2.5 equiv of THF, in the case of the less reactive amido complex [La{$N(SiMe_3)_2$}$_3$] a large excess of THF was required to obtain (*R*)-**4b** as the sole product.[25] Furthermore, removal of solvent from (*R*)-**4b** led to the formation of a yet unidentified second species.[26,27]

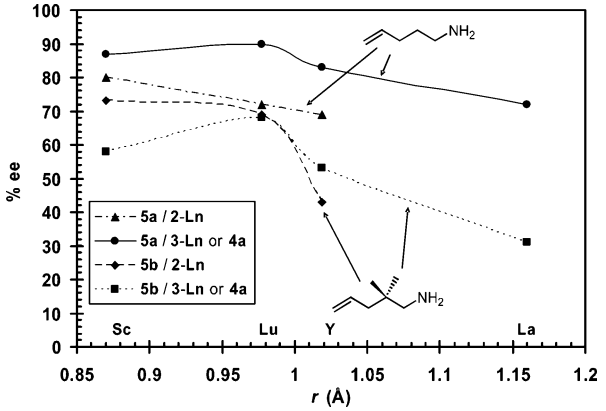

Figure 1. Ionic radius dependence of enantiomeric excess for pyrrolidines obtained from aminopentenes **5a** and **5b** with binaphtholate catalysts (*R*)-**2-Ln**, (*R*)-**3-Ln** (Ln = Sc, Lu, Y), and (*R*)-**4a**. The lines are drawn as a guide for the eye.

Asymmetric Hydroamination of Aminoalkenes. All binaphtholate complexes displayed high catalytic activity at room temperature in the hydroamination/cyclization of aminopentenes **5a**−**d**, while aminohexenes **7a** and **7b** required elevated reaction temperatures (Table 1). Complexes based on the smallest rare earth metal, scandium, were less active and required higher reaction temperatures (in some cases) to achieve appreciable turnover frequencies. Catalytic activity increased with increasing ionic radius. The lanthanum catalyst (*R*)-**4a** displayed the highest turnover rates for the unactivated aminopentene **5a** (37 h^{-1} at 22 °C) and the *gem*-dimethyl-substituted **5b** (94 h^{-1} at 22 °C). Cyclization of **5c** proceeded with rates as high as 840 h^{-1} at 25 °C using (*R*)-**2-Y**, as a result of the significant Thorpe−Ingold effect[28] of the *gem*-diphenyl substituents.

Enantioselectivity of the pyrrolidine products generally increased with decreasing ionic radius of the metal (see trends for **5a** and **5b** in Figure 1). **5a** and **5b** were cyclized more efficiently (with respect to rate and enantioselectivity) using the sterically more hindered tris(3,5-xylyl)silyl-substituted binaphtholate complexes (*R*)-**3-Ln** in comparison to using the corresponding triphenylsilyl-substituted binaphtholate complexes (*R*)-**2-Ln** of the same rare earth metal. The opposite trend was observed for the sterically more demanding substrates **5c** and **5d**. An exception in this series of complexes was the scandium complex (*R*)-**3-Sc**, as it displayed generally lower selectivity and slower rates than (*R*)-**2-Sc** and the lutetium complex (*R*)-**3-Lu**, most likely due to steric overcrowding of the coordination sphere around scandium.

Interestingly, the most reactive substrate **5c** was also cyclized with the highest selectivity (up to 95% ee using (*R*)-**2-Sc**). The less reactive aminopentene **5a** was cyclized in 92% ee using

(19) (a) Ln = Y: Booij, M.; Kiers, N. H.; Heeres, H. J.; Teuben, J. H. *J. Organomet. Chem.* **1989**, *364*, 79. (b) Ln = Lu: Wayda, A. L.; Rogers, R. D. *Organometallics* **1985**, *4*, 1440. (c) Ln = Sc: Manzer, L. E. *J. Am. Chem.* Soc. **1978**, *100*, 8068.

(20) (a) Maruoka, K.; Itoh, T.; Araki, Y.; Shirasaka, T.; Yamamoto, H. *Bull. Chem. Soc. Jpn.* **1988**, *61*, 2975. (b) Gong, L.-Z.; Pu, L. *Tetrahedron Lett.* **2000**, *41*, 2327.

(21) The complexes were commonly obtained as glassy solids after removal of the solvent. Precipitation from pentane or hexanes did not improve the purity of the complexes, and we have thus far been unable to obtain single crystals suitable for X-ray crystallographic analysis. Also, derivatization of complexes (*R*)-**2** and (*R*)-**3** either via substitution of the coordinated *N*,*N*-dimethylbenzylamine by other donors (e.g., Et_2O, THF) or by protonolysis of the yttrium−aryl bond with an amine (e.g., $HN(SiMe_3)_2$, $HN(CH_2CH_2OMe)_2$) did not lead to a better isolable product.

(22) Reaction of (*R*)-**2-Y** with 2 equiv *n*-propylamine also led to a replacement of the coordinated *N*,*N*-dimethylbenzylamine, concomitant with rapid protolytic cleavage of the yttrium−aryl bond and formation of a diolate amido amine species.

(23) (a) Hitchcock, P. B.; Lappert, M. F.; Smith, R. G.; Bartlett, R. A.; Power, P. P. *J. Chem. Soc., Chem. Commun.* **1988**, 1007. (b) Bradley, D. C.; Ghotra, J. S.; Hart, F. A. *J. Chem. Soc., Dalton Trans.* **1973**, 1021.

(24) We have been unable to generate the corresponding enantiopure triphenylsilyl binaphtholate lanthanum complex cleanly starting from (*R*)-**1a** and [La{$CH(SiMe_3)_2$}$_3$] under the conditions reported by Schaverien for the corresponding racemic complex.[18]

(25) Reaction of [La{$N(SiMe_3)_2$}$_3$] and (*R*)-**1b** in the absence of THF or in the presence of only a few equivalents of THF led to the formation of a species which did not contain any amido ligand and which we therefore assign to be of dimeric or oligomeric nature with more than one binaphtholate ligand per metal center. Also, [La{$CH(SiMe_3)_2$}$_3$] and (*R*)-**1b** did not form a clean product in the absence of THF.

(26) The close proximity of several aromatic substituents suggest that one of the aromatic rings of the trisarylsilyl binaphtholate ligands could form a π-arene complex with the metal center as a result of partial loss of THF. For a review on π-arene rare earth metal complexes see: Bochkarev, M. N. *Chem. Rev.* **2002**, *102*, 2089.

(27) Note that addition of aminoalkene substrate to this mixture of two species generated a single catalytically active species, which was presumably identical to that formed from the corresponding bis(THF) adduct of the precatalyst.

(28) Jung, M. E.; Pizzi, G. *Chem. Rev.* **2005**, *105*, 1735.

(29) Ringdahl, B.; Pereira, W. E., Jr.; Craig, J. C. *Tetrahedron* **1981**, *37*, 1659.

Table 1. Catalytic Hydroamination/Cyclization of Aminoalkenes

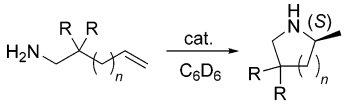

5a *n* = 1, R = H
5b *n* = 1, R = Me
5c *n* = 1, R = Ph
5d *n* = 1, R-R = -$(CH_2)_4$-
7a *n* = 2, R = H
7b *n* = 2, R = Me

6a *n* = 1, R = H
6b *n* = 1, R = Me
6c *n* = 1, R = Ph
6d *n* = 1, R-R = -$(CH_2)_4$-
8a *n* = 2, R = H
8b *n* = 2, R = Me

entry	cat.	substrate	[cat.]/[subst.] (%)	*T* (°C)	*t* (h)	yield (%)[a]	N_t (h^{-1})	ee (%)[b]
1	(*R*)-**2-Sc**	**5a**	2	60	96	96	0.5	80
2	(*R*)-**3-Sc**	**5a**	2	60	27	95	1.5	87
3	(*R*)-**2-Lu**	**5a**	2	60	4	96	18	72
4	(*R*)-**3-Lu**	**5a**	5	22	16.5	93	1.7	90
5	(*R*)-**3-Lu**	**5a**	4	0[c]	190	92	0.13	92
6	(*R*)-**2-Y**	**5a**	2	25	24	95	2.6	70
7	(*R*)-**2-Y**	**5a**	2	60	0.8	95	93	66
8	(*R*)-**2-Y**+ 3 THF	**5a**	1	22	53.5	96	2.0	70
9	(*R*)-**3-Y**	**5a**	4	22	20	94	2.2	83
10	(*R*)-**4a**	**5a**	3	22	1.4	89	37	72
11	(*R*)-**4b**	**5a**	1.7	22	5.5	95	≥ 33	71
12	(*R*)-**2-Sc**	**5b**	2	60	5.5	93	13	73
13	(*R*)-**3-Sc**	**5b**	2	22	192	91	0.3	58
14	(*R*)-**3-Sc**	**5b**	2.5	60	10.5	94	5.5	56
15	(*R*)-**2-Lu**	**5b**	2	22	27.5	94	2.4	69
16	(*R*)-**3-Lu**	**5b**	3	22	14	95	3.1	68
17	(*R*)-**2-Y**	**5b**	4	22	3	95	8	43
18	(*R*)-**2-Y**	**5b**	3	60	0.07	92	480	65
19	(*R*)-**2-Y** + 3 THF	**5b**	1.5	22	22	95	5.6	38
20	(*R*)-**2-Y** + 300 THF[d]	**5b**	2	22	24	94	2.1	31
21	(*R*)-**3-Y**	**5b**	4	22	2	95	14	53
22	(*R*)-**4a**	**5b**	3.5	22	0.45	95	94	31
23	(*R*)-**4b**	**5b**	1	22	5	95	≥ 60	24
24	(*R*)-**2-Sc**	**5c**	2	25	0.6	94	110	95
25	(*R*)-**3-Sc**	**5c**	2	25	3	96	20	74
26	(*R*)-**2-Lu**	**5c**	2	25	0.25	96	≥ 180	93
27	(*R*)-**3-Lu**	**5c**	2	25	0.1	96	≥ 500	80
28	(*R*)-**2-Y**	**5c**	2	25	0.06	96	≥ 840	84
29	(*R*)-**3-Y**	**5c**	2	25	0.06	94	≥ 760	77
30	(*R*)-**2-Sc**	**5d**	2	25	6	97	11	85
31	(*R*)-**3-Sc**	**5d**	2	25	13	96	5.0	61
32	(*R*)-**2-Lu**	**5d**	2	25	0.11	95	460	83
33	(*R*)-**3-Lu**	**5d**	2	25	0.5	95	100	78
34	(*R*)-**2-Y**	**5d**	2	25	0.2	97	420	63
35	(*R*)-**3-Y**	**5d**	2	25	0.3	97	240	69
36	(*R*)-**2-Sc**	**7a**	2	80	84	95	0.65	16
37	(*R*)-**3-Sc**	**7a**	2	80	23	94	2.2	43
38	(*R*)-**2-Lu**	**7a**	2	80	14	95	4.0	40
39	(*R*)-**3-Lu**	**7a**	2	80	21	94	2.1	55
40	(*R*)-**3-Y**	**7a**	2	80	40	92	1.6	46
41	(*R*)-**2-Sc**	**7b**	2	60	20	97	4.1	40
42	(*R*)-**3-Sc**	**7b**	2	60	64	97	0.9	61
43	(*R*)-**2-Lu**	**7b**	2	60	7.5	96	6.4	42
44	(*R*)-**3-Lu**	**7b**	2	60	7.5	97	6.8	40
45	(*R*)-**3-Y**	**7b**	2	60	20	97	2.9	36

[a] NMR yield determined relative to ferrocene internal standard. [b] Enantiomeric excess determined by ^{19}F NMR of Mosher amides. Pyrrolidines prepared with (*R*)-binaphtholate catalysts have (*S*) configuration according to the X-ray crystallographic analysis of the Mosher amide of (*S*)-**6c** (Supporting Information) and the observed positive ORD for **6a** and **6b**. $[\alpha]^{20}_D = -20.0°$ for (*R*)-**6a**, see ref 29. $[\alpha]^{20}_D = -24.3°$ for (*R*)-**6b**, see ref 9b. [c] In toluene-d_8. [d] Substrate: THF = 1:6.

(*R*)-**3-Lu** at 0 °C (90% ee at 22 °C). Overall, the enantiomeric excess of pyrrolidines **5a** and **5c** depended only slightly on the reaction temperature (Δee ≈ 1.5% ee/10 °C in the range of 0−60 °C for **5a**, Figure S4).[30] However, it is noteworthy that the enantiomeric excess of **6b** increased with increasing temperature using (*R*)-**2-Y** as catalyst to level out at a maximum value of 66% ee at 100 °C (Figure S9),[30] concomitant with the observation of increased rates after about the first half-life (vide infra).

The (*R*)-binaphtholate catalysts furnished the pyrrolidine products preferentially with (*S*) configuration.[31] Similar to lanthanocene catalyst systems,[8b] the catalytic activity of binaphtholate rare earth metal complexes was affected only slightly by the addition of THF, which is indicative of a stronger binding of the aminoalkene substrate in comparison to ethereal donors. Furthermore, catalyst enantioselectivity was affected markedly only in the presence of a large excess of THF (Table 1, entry 20).

(30) See Supporting Information for details.

(31) See X-ray crystallographic analysis of the Mosher amide of **6c** in the Supporting Information.

Table 2. Catalytic Hydroamination/Cyclization of Aminoalkenes

Entry	Substrate	Product	cat.	[cat.]/[subst.] in %	*T* (°C)	*t* (h)	Yield in %[a]	N_t (h^{-1})	% ee (dr)
1	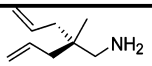	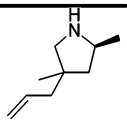	(*R*)-**2-Sc**	2	22	23	93	3	88, 78 (2.7:1)
2	**9**	**10**	(*R*)-**2-Lu**	2	22	0.8	94	80	86, 76 (2.3:1)
3			(*R*)-**3-Lu**	1	22	1.6	95	67	77, 74 (1.6:1)
4			(*R*)-**2-Y**	2	22	1	95	75	63, 53 (1.8:1)
5			(*R*)-**3-Y**	2	22	1.2	94	70	65, 65 (1.4:1)
6	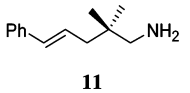	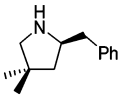	(*R*)-**2-Sc**	2	100	72	91	0.6	72
7	**11**	**12**	(*R*)-**2-Lu**	2	60	10	98	4.0	67
8			(*R*)-**3-Lu**	2	60	28	96	2.3	23
9			(*R*)-**3-Y**	2	60	23	96	2.1	25
10	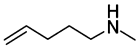	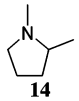	(*R*)-**2-Sc**	2	60	76	94	0.7	33
11	**13**	**14**	(*R*)-**3-Sc**	2	60	44	93	0.9	53
12			(*R*)-**3-Lu**	2	25	120	96	1	17
13			(*R*)-**2-Y**	2	60	2.3	96	35	2

[a] NMR yield determined relative to ferrocene internal standard.

Whereas pyrrolidines **6a**−**d** were formed quite selectively using the binaphtholate catalysts **2-Ln** and **3-Ln**, cyclization of aminohexenes **7a** and **7b** produced piperidines **8a** and **8b** with moderate selectivity (up to 55% ee for **8a** using (*R*)-**3-Lu**, up to 61% ee for **8b** using (*R*)-**3-Sc**).

Cyclization of the aminodiolefin **9** (Table 2) proceeded with high selectivity using (*R*)-**2-Sc** (88 and 78% ee) but only low diastereoselectivity (2.7:1). Interestingly, the minor diastereomer of pyrrolidine **10** exhibited a significantly lower enantiomeric excess than the major diastereomer for all triphenylsilyl-substituted binaphtholate complexes (*R*)-**2-Ln**, while both diastereomers where obtained with essential identical enantiomeric excess using tris(3,5-xylyl)silyl-substituted binaphtholate complexes (*R*)-**3-Ln**. The triphenylsilyl-substituted binaphtholate complexes were also more successful in the cyclization of the 1,2-disubstituted olefin **11** (Table 2, entries 6, 7). Steric congestion around nitrogen, as found in the secondary aminoalkene **13**, resulted in significantly reduced selectivities in comparison to that of the primary aminoalkene analogue **5a**, and only the scandium catalysts gave an appreciable enantiomeric excess.

Further evidence for the high catalytic activity of diolate rare earth metal hydroamination catalysts provided the *anti*-Markovnikov[32] addition of *n*-propylamine to styrene mediated by the lanthanum complex **4a** with an initial turnover frequency of 0.7 h^{-1} ([styrene] = 0.8 mol L^{-1}) at 60 °C (eq 3).

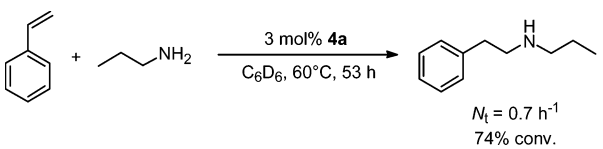

(3)

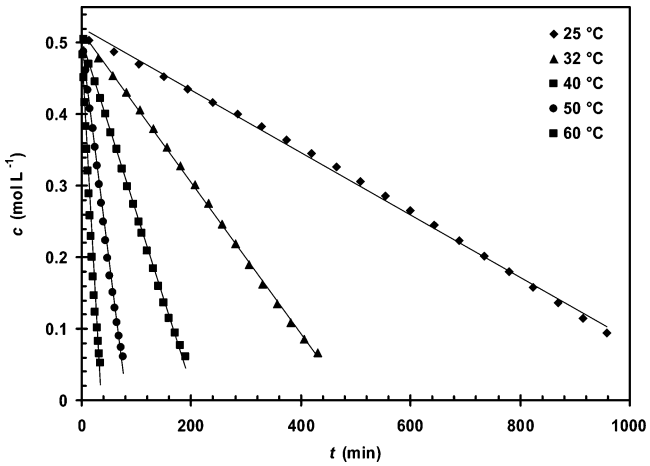

Figure 2. Time dependence of substrate concentration in the hydroamination/cyclization of **5a** ([subst.]$_0$ = 0.50 mol L^{-1}) with (*R*)-**2-Y** ([Ln] = 0.01 mol L^{-1}) at variable temperatures in C_6D_6. The lines through the data points represent the least-squares fit for all data.

Kinetics of Hydroamination/Cyclization. In accordance with the generally accepted mechanism of hydroamination/cyclization,[8b] in which the olefin insertion step is rate determining, most reactions showed apparent zero-order rate dependence on substrate concentration up to three half-lives for a given initial substrate concentration (Figure 2). Some plots showed a slight curvature (Figure S5, see also Figure 6),[30] indicating a slight rate acceleration during the catalytic reaction prior the onset of

(32) Rare earth and alkali metal catalyzed hydroamination reactions of vinyl arenes generally proceed with *anti*-Markovnikov selectivity,[2b,f,10] whereas late transition metals[2h,7a] or Broenstedt acid catalysts furnish the Markovnikov products; see: (a) Anderson, L. L.; Arnold, J.; Bergman, R. G. *J. Am. Chem. Soc.* **2005**, *127*, 14542. (b) Kaspar, L. T.; Fingerhut, B.; Ackermann, L. *Angew. Chem., Int. Ed.* **2005**, *44*, 5972.

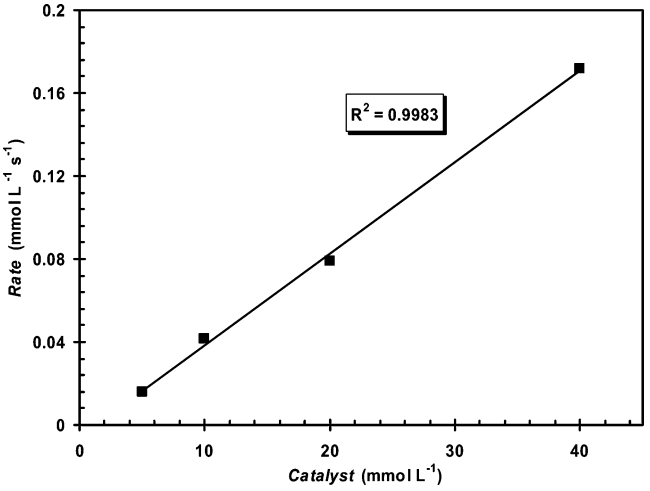

Figure 3. Rate dependence on catalyst concentration for the hydroamination/cyclization of **5a** ([subst.]$_0$ = 0.50 mol L^{-1}) with (*R*)-**2-Y** in C_6D_6 at 40 °C.

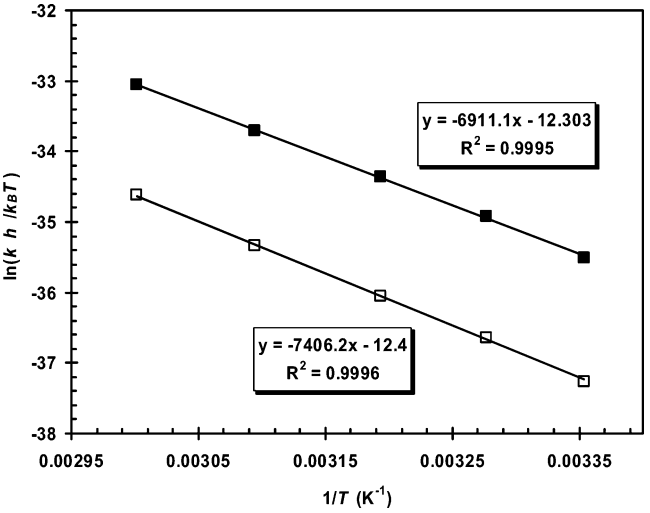

Figure 4. Eyring plot for the hydroamination/cyclization of **5a** ([subst.]$_0$ = 0.50 mol L^{-1}, k_R: □, k_S: ■) using (*R*)-**2-Y** ([Ln] = 0.01 mol L^{-1}). The rate constants k_R and k_S were determined according to $k_R = k_1(1 - ee)/2$ and $k_S = k_1(1 + ee)/2$.

product inhibition observed at high conversion (>85% conversion). However, catalyst activation (= protonolysis of Ln−X by the aminoalkene substrate, where X is an alkyl, aryl, or amido substituent) was generally instantaneous and irreversible, except in the case of the amido complex **4b**, where the precatalyst is regenerated at high conversions concomitant with a decrease in the rate of cyclization. The first-order rate dependence on catalyst concentration over an 8-fold range (Figure 3) is indicative of a monomeric catalytically active species.

The activation parameters for the lower transition state leading to pyrrolidine (*S*)-**6a** ($\Delta H(S)^{\ddagger}$ = 57.4(0.8) kJ mol^{-1} and $\Delta S(S)^{\ddagger}$ = −102(3) J K^{-1} mol^{-1}) and the activation parameters for the higher transition state leading to pyrrolidine (*R*)-**6a** ($\Delta H(R)^{\ddagger}$ = 61.5(0.7) kJ mol^{-1} and $\Delta S(R)^{\ddagger}$ = −103(3) J K^{-1} mol^{-1}) were obtained from the Eyring plot (Figure 4). They are in good agreement with the activation parameters reported by Marks for the achiral lanthanocene catalyst [Cp*$_2$LaCH(SiMe$_3$)$_2$] ($\Delta H^{\ddagger}$ = 12.7(1.4) kcal mol^{-1} ≅ 53(6) kJ mol^{-1}, $\Delta S^{\ddagger}$ = −27(4.6) eu ≅ −113(19) J K^{-1} mol^{-1}),[8b] indicating that the hydroamination/cyclization involves a similar highly ordered transition state as

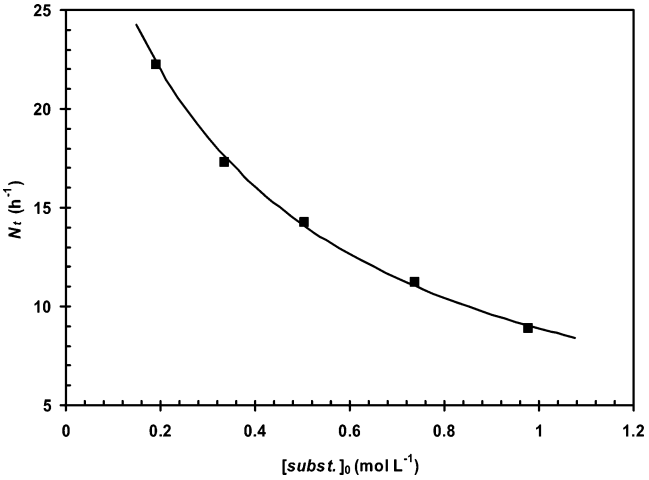

Figure 5. Dependence of turnover frequency (N_t) on initial substrate concentration ([subst.]$_0$) in the cyclization of **5a** with (*R*)-**2-Y** ([Ln] = 0.02 mol L^{-1}) at 40 °C. The line represents the best fit for k_1 = 29.7(1.2) h^{-1} and K^{dorm} = 2.50(0.12) mol^{-1} L.[30]

Scheme 2

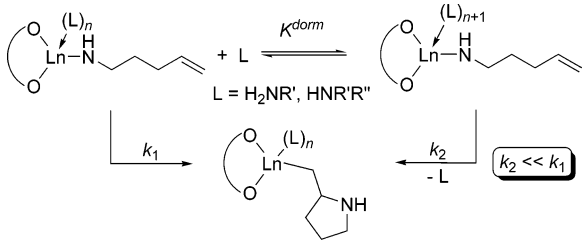

proposed for the lanthanocene catalysts. The two diastereomeric cyclization transition states differ by $\Delta\Delta H^{\ddagger}$ = 4.1(0.8) kJ mol^{-1} in their activation enthalpies, but show essentially the same degree of order ($\Delta\Delta S^{\ddagger}$ = 1(3) J K^{-1} mol^{-1}).

The signals of **5a** in the ^{1}H NMR spectra of catalytic experiments showed significant line broadening as well as an upfield shift of the α- and β-methylene protons (Figure S7, trace d), which increased with increasing conversion,[30] indicating a strong binding of the substrate to the metal center and a fast exchange on the NMR time scale between coordinated amine and amido ligands and free amine.[33] The signals of the product heterocycle **6a** showed a similar line broadening (Figure S7, trace d).[30]

Although the reactions show an apparent zero-order rate dependence on substrate concentration, decreasing reaction rates were observed with increasing initial substrate concentrations (Figure 5).[34] The reactions are impeded by the presence of coordinating bases, but the observation of an apparent zero-order rate dependence on substrate concentration suggests that the starting aminoalkene and pyrrolidine product bind with equilibrium constants of similar order of magnitude to the metal center (Scheme 2), at least for the substrate/catalyst combination discussed herein.[35]

The rate depression was also clearly visible when the substrate was added in two batches (Figure 6). Cyclization of **5a** (0.50 mol L^{-1}) in the presence of product heterocycle **6a** (0.50 mol L^{-1}) with (*R*)-**2-Y** (0.02 mol L^{-1}) showed a reduced rate (8.4 h^{-1} vs 15.0 h^{-1} for the first run in the absence of **6a**) of apparent zeroth order.[34b]

(33) In catalytic and stoichiometric experiments no discrete catalyst species could be observed.

Therefore, the rate law for the catalytic hydroamination/cyclization of aminoalkenes using binaphtholate rare earth metal catalysts can be approximated by eq 5, with L being the combined concentrations of amine bases and K^{dorm} the equilibrium constant between the catalytically active amido amine species and the dormant amido diamine species (vide infra).[36] The experimental values for the turnover frequencies N_t (N_t = rate/[Ln]) plotted vs the initial concentration of substrate were approximated with eq 5[30] to give $k_1 = 29.7(1.2)$ h^{-1} and $K^{dorm} = 2.50(0.12)$ mol^{-1} L at 40 °C, respectively $k_1 = 113(4)$ h^{-1} and $K^{dorm} = 0.89(0.06)$ mol^{-1} L at 60 °C.

$$\text{rate} = -\frac{\text{d[subst.]}}{\text{d}t} = \frac{k_1[\text{Ln}]}{1 + K^{\text{dorm}}[\text{L}]} \qquad (5)$$

High substrate concentrations were also slightly detrimental to product enantioselectivity. Cyclization of **5a** using (*R*)-**2-Y** proceeded with 72% ee in a dilute substrate solution ([subst.]$_0$ = 0.19 mol L^{-1}), while a concentrated solution furnished **6a** in only 68% ee ([subst.]$_0$ = 0.98 mol L^{-1}, [Ln] = 0.02 mol L^{-1} in both cases). However, the enantiomeric excess of **6a** prepared with (*R*)-**2-Y** was invariant at various extents of conversion, and no influence of catalyst concentration on product enantioselectivity was observed.

Cyclization of **5b** with (*R*)-**2-Y** showed significantly more pronounced rate acceleration than observed for **5a** (Figure S8),[30] indicating a stronger substrate inhibition and weaker binding of the product heterocycle **6b** to the metal center for this substrate/catalyst combination. Concomitant to these observations the enantiomeric excess increased with increasing reaction temperature (vide supra and Figure S9).

Cyclization of the nitrogen deuterated substrate **5a**-d_2 proceeded significantly more slowly than the non-deuterated **5a** (3.6 h^{-1} at 40 °C for **5a**-d_2 vs 15 h^{-1} for **5a** using 4 mol % (*R*)-**2-Y**, [Ln] = 0.02 mol L^{-1}), indicating a primary kinetic isotope effect of 4.2. This kinetic isotope effect is comparable to the value of 2.7 observed for [Cp*$_2$LaCH(SiMe$_3$)$_2$] at 60 °C.[8b] However, enantioselectivity was not affected (70% ee for **6a**-d_2 vs 69% ee for **6a**). Furthermore, cyclization was irreversible at room temperature, as neither the isotopic substitution pattern in **6a**-d_2 nor the enantiomeric excess changed after 45 days at 25 °C.

Kinetic Resolution of Chiral Aminoalkenes. The catalytic kinetic resolution is an important methodology in organic synthesis for the preparation of enantioenriched compounds.[37] Kinetic resolution of chiral aminoalkenes via asymmetric hydroamination on the other hand has not been performed successfully prior to our studies.[17,38] Attempts to resolve **15a** with chiral lanthanocene complexes gave only low enantiomeric excess (<20% ee) at various extents of conversion.[9b] However, binaphtholate catalysts **2**−**4** were successfully employed in the kinetic resolution of chiral aminoalkenes (Table 3, Figure 7) with a resolution factor f ($f = K^{dias}(k_{fast}/k_{slow})$, vide infra) of up to 19.

A simple protocol allowed the convenient separation of aminoalkene starting material and pyrrolidine product by aqueous extraction of the secondary ammonium acetate from the benzaldimine of the primary amine (Scheme 3).

The resolution factor for the sterically least demanding methyl-substituted substrate **15a** increased slightly in the order Lu ≤ Y < Sc using triphenylsilyl-substituted binaphtholate catalysts (*R*)-**2-Ln** and had a maximum value of 12 for catalyst (*R*)-**2-Sc** with the smallest rare earth element. The sterically more encumbered binaphtholate complexes (*R*)-**3-Ln** were

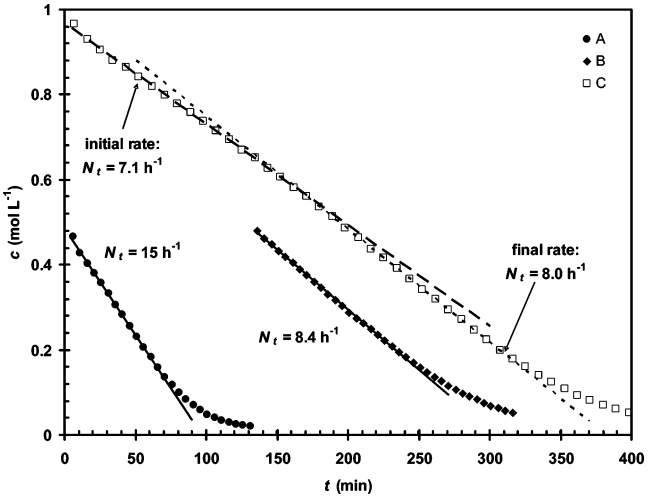

Figure 6. Time dependence of substrate concentration in the hydroamination/cyclization of **5a** using (*R*)-**2-Y** ([Ln] = 0.02 mol L^{-1}) at 40 °C. A) First run ([subst.]$_0$ = 0.50 mol L^{-1}). B) Second run with a second batch of substrate **5a** ([subst.]$_0$ = 0.50 mol L^{-1}) added. C) Independent kinetic run with [subst.]$_0$ = 1.00 mol L^{-1}. The lines through the data points represent the least-squares fit for the linear part of the data.

(34) (a) In catalytic experiments with [Cp*$_2$LaCH(SiMe$_3$)$_2$] we did not observe a rate dependence on overall substrate concentration within the margin of experimental error under the same reaction conditions. Furthermore, the ^{1}H NMR signals of the substrate and product remained sharp throughout the catalytic experiments, indicating a significant weaker binding of the amine bases to the sterically more hindered metallocene complex in comparison to the sterically more accessible binaphtholate catalysts. (b) Marks observed a similar rate depression in the cyclization of an aminodiene substrate using a constrained geometry catalyst,[9d] indicating a substantial binding of the heterocyclic product to the metal center.

(35) (a) Other substrate/catalyst combinations can have different binding constants for substrate and product, as the increased rates observed at high conversion in the cyclization of **5b** using (*R*)-**2-Y** indicate (Figure S8). (b) Variable-temperature NMR studies of reaction mixtures containing (*R*)-**2-Y** and 3 equiv of **6a** in toluene-d_8 showed broad features over a large temperature range (−60 to +80 °C), even in the presence of the noncyclizable primary amine *n*-propylamine (see Figures S1 and S2).[30] No decoalescence was observed even at −90 °C.

(36) (a) The presence of coordinating bases to the catalytically active species has been argued by Marks and co-workers for lanthanocene complexes based on kinetic and mechanistic studies (e.g. effects of exogenous bases on reaction rates and diastereoselectivity, paramagnetic line broadening of substrate and product signals in the NMR spectra of catalytic hydroamination reactions, kinetic isotope effects).[8b,9b] (b) The number of amines coordinated to species **A** and **B** (see Scheme 6) could not be determined yet, as these species could not be observed independently by NMR spectroscopy.[33] However, on the basis of the preference of diolate rare earth metal complexes to form five-coordinate complexes (e.g. in complexes **2** and **3**, see also ref 16a) we believe species **B** to be a coordinatively saturated diamine amido complex, while species **A** should possess an empty coordination site required for the olefin insertion step. This proposal would also be in agreement with the significantly reduced catalytic activity observed for diolate diamine complexes.[15a,e,f] (c) [L] = [subst.] + [pyrrolidine] ≈ [subst.]$_0$ −3 [Ln]. Three equivalents of amine are consumed per molecule of precatalyst in the formation of the amido diamine species **B** (Scheme 6), which is thought to be the dominant resting state of the catalyst in solution in the presence of a large excess of amine bases.[30]

(37) (a) Kagan, H. B.; Fiaud, J. C. *Top. Stereochem.* **1988**, *18*, 249. (b) Keith, J. M.; Larrow, J. F.; Jacobsen, E. N. *Adv. Synth. Catal.* **2001**, *343*, 5. (c) Kagan, H. B. *Tetrahedron* **2001**, *57*, 2449. (d) Vedejs, E.; Jure, M. *Angew. Chem., Int. Ed.* **2005**, *44*, 3974.

(38) Chiral amines can be resolved efficiently via enzymatic acylation; see: (a) v. Rantwijk, F.; Sheldon, R. A. *Tetrahedron* **2004**, *60*, 501. For nonenzymatic kinetic resolutions of amines, see: (b) Arai, S.; Bellemin-Laponnaz, S.; Fu, G. C. *Angew. Chem., Int. Ed.* **2001**, *40*, 234. (c) Al-Sehemi, A. G.; Atkinson, R. S.; Fawcett, J.; Russell, D. R. *Tetrahedron Lett.* **2000**, *41*, 2239. (d) Miyano, S.; Lu, L. D.-L.; Viti, S. M.; Sharpless, K. B. *J. Org. Chem.* **1985**, *50*, 4350. Preparation of chiral amines via asymmetric imine hydrogenation and hydrosilylation: (e) Viso, A.; Lee, N. E.; Buchwald, S. L. *J. Am. Chem. Soc.* **1994**, *116*, 9373. (f) Yun, J.; Buchwald, S. L. *J. Org. Chem.* **2000**, *65*, 767.

Table 3. Catalytic Kinetic Resolution of Chiral Aminopentenes[a]

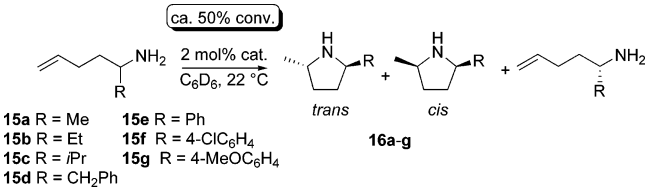

entry	catalyst	substrate	*t* (h)	conversion (%)	% yield of SM; prod.[b]	*trans*:*cis*	recovered **15:** ee (%)	**16**: ee (%)	*f*[c]
1	(*R*)-**2-Sc**	**15a**	94[d]	51	39; 45	10:1	73	64	12
2	(*R*)-**3-Sc**	**15a**	94[d]	50	38; 44	7:1	73	71	14
3	(*R*)-**2-Lu**	**15a**	42	55	37; 50	10:1	73	58	8.4
4	(*R*)-**3-Lu**	**15a**	24.5	51	38; 47	9:1	75	73	14
5	(*R*)-**2-Y**	**15a**	25.5	53	39; 49	11:1	72	68	9.5
6	(*R*)-**2-Y**+2 THF	**15a**	15	52	40; 47	8:1	68	58	8.7
7	(*R*)-**3-Y**	**15a**	26	52	39; 46	13:1	80	78 (−)[e]	16
8	(*R*)-**4b**[f]	**15a**	25	50	40; 44	7:1	65	73	9.1
9	(*R*)-**2-Y**[g]	**15b**	4.5	51	42; 47	16:1	51	−	4.7
10	(*R*)-**3-Y**[g]	**15b**	6	51	39; 46	20:1	57	−	5.9
11	(*R*)-**2-Y**[f]	**15c**	6	50.5	40; 49	18:1	37	−	3.0
12	(*R*)-**3-Y**[f]	**15c**	24	51	46; 47	7:1	44	−	3.7
13	(*R*)-**2-Y**[f]	**15d**	9	50	45; 39	20:1	42	40 (−)	3.6
14	(*R*)-**3-Y**	**15d**	27	52	44; 46	20:1	38	34	2.9
15	(*R*)-**2-Lu**	**15e**	15[d]	52	42; 51	≥50:1	83	−	19
16	(*R*)-**3-Lu**[f]	**15e**	40	52	46; 51	≥50:1	59	−	6
17	(*R*)-**2-Y**	**15e**	95	50	47; 41	≥50:1	74[h]	63 (+)[i]	15
18	(*R*)-**3-Y**	**15e**	18[d]	52	41; 50	≥50:1	63	−	7
19	(*R*)-**2-Y**	**15f**	18[d]	50	44; 48	≥50:1	71	−	12
20	(*R*)-**2-Y**	**15g**	8[d]	50	43; 47	≥50:1	78	−	19

[a] Reaction conditions: 2 mol % cat., C_6D_6, Ar atm, 22 °C. [b] Isolated yield of starting material (SM) and product. Volatile amines were isolated as hydrochloride salts. [c] Resolution factor $f = K^{dias} \times k_{fast}/k_{slow}$. [d] At 40 °C. [e] A (−) optical rotation corresponds to a (2*S*,5*S*) absolute configuration, see ref 39. [f] 1.5 mol % cat. [g] 1.0 mol % cat. [h] $[\alpha]^{22}_D = +12.9°$ for enantiopure (*S*)-**15e**·HCl, $[\alpha]^{22}_D = -41.9°$ for (2*R*,5*S*)-**16e**. [i] Determined by chiral HPLC.

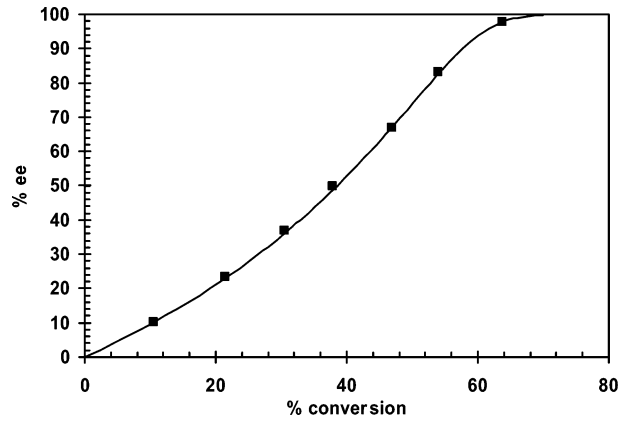

Figure 7. Dependence of enantiomeric excess of recovered starting material on conversion in the kinetic resolution of **15e** with (*R*)-**2-Y** at 30 °C. The line was fitted using eq 12 to a resolution factor $f = 14.5$.[30]

consistently more efficient for **15a** with resolution factors as high as 16 for the middle sized yttrium, while (*R*)-**4b** with the larger lanthanum metal was the least effective resolution catalyst. Addition of THF was slightly detrimental for diastereoselectivity and kinetic resolution of **15a** (Table 3, entry 6). Both series of catalysts, (*R*)-**2-Ln** and (*R*)-**3-Ln**, exhibited similar catalytic activity in cyclization of **15a**, which increased with increasing ionic radius of the metal.

Substrates with sterically more demanding α-alkyl substituents were increasingly less efficiently kinetically resolved, although again the sterically more hindered (*R*)-**3-Y** was slightly more effective than (*R*)-**2-Y**. The resolution factors decreased in the following sequence of substrates: **15a** (R = Me, Table 3, entries 5 and 7) > **15b** (R = Et, entries 9 and 10) > **15c** (R = *i*Pr, entries 11 and 12) ≈ **15d** (R = CH_2Ph, entries 13 and 14). However, aryl-substituted substrates **15e**−**g** were more efficiently resolved using catalysts (*R*)-**2-Ln** (Ln = Lu, Y, Table 3, entries 15, 17, 19, and 20) having the sterically less demanding 3,3′-bis(triphenylsilyl)-substituted binaphtholate ligand.

Scheme 3 [a]

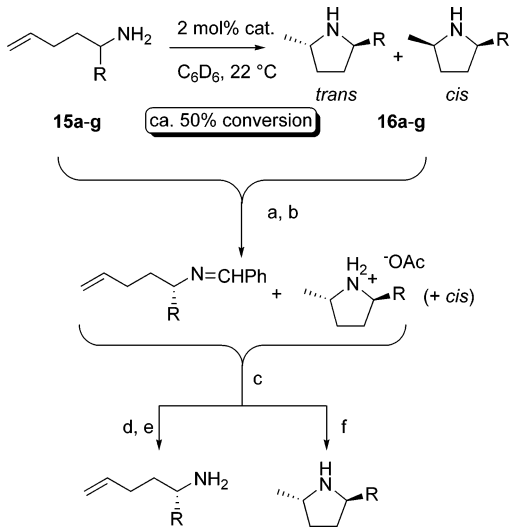

[a] Reagents and conditions: (a) 0.55 equiv AcOH; (b) 0.6 equiv PhCHO, 25 °C, 2 h; (c) extraction with benzene/hexanes/water (1/1/2); (d) organic layer: 2N HCl, Et_2O, 25 °C, 24 h; (e) aq NaOH; (f) aqueous layer: aq NaOH.

The 2,5-disubstituted pyrrolidines were obtained in moderate to excellent *trans* diastereoselectivity, depending on the steric hindrance of the α-substituent. Diastereoselectivity for methyl-

Scheme 4

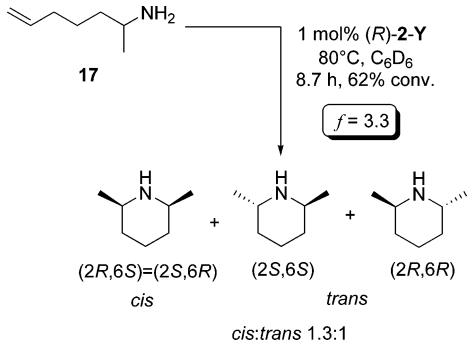

substituted **15a** ranged from 7:1 for catalysts (*R*)-**3**-**Sc** and (*R*)-**4b**, up to 13:1 for (*R*)-**3**-**Y**. Sterically more demanding alkyl-substituted substrates **15b**−**15d** exhibited higher *trans*/*cis* selectivities (*trans*/*cis* = 16:1−20:1, except for entry 12). The highest diastereoselectivity was observed for aryl-substituted substrates **15e**−**g**, which gave consistently high *trans*/*cis* selectivities ≥50:1.

Resolution of *p*-chlorophenyl-substituted **15f** occurred with (*R*)-**2**-**Y** slightly less efficient than resolution of **15e**, whereas a higher selectivity was observed for the *p*-methoxyphenyl-substituted **15g**. Interestingly, the presence of the methoxy group in **15g** did not diminish the rate of cyclization. In fact, cyclization of **15g** proceeded at least twice as fast as **15f**. These examples indicate that the electron density at the aromatic ring influences the rate as well as selectivity of cyclization.

Kinetic resolution of **15e** using 1 mol % (*R*)-**2**-**Lu** gave enantiopure (*S*)-**15e** (≥99% ee) in 33% re-isolated yield at 64% conversion. The absolute configuration was determined by X-ray crystallographic analysis of the ring-closed pyrrolidine hydrochloride (2*R*,5*S*)-**16e**·HCl (Supporting Information) prepared with (*S*)-**2**-**Y**. Therefore, in agreement with observations made for substrates **5a**−**5d**, the cyclization of chiral aminoalkenes **15a**−**15g** proceeds with (*R*)-binaphtholate catalysts preferentially through an approach of the Ln−N bond to the *re* face of the olefin.

Kinetic resolution of 1-methylhex-5-enylamine (**17**) required elevated temperature and exhibited a low resolution factor for (*R*)-**2**-**Y** as well as a poor *cis*/*trans* ratio for the piperidine product. (Scheme 4).

Kinetics of the Resolution Process. According to the general model for the kinetic resolution of aminoalkenes (Scheme 5) the total amount of catalyst [Ln] is distributed among two substrate/catalyst complexes [cat.−R] and [cat.−S] (eq 6), which readily interconvert in the presence of both enantiomers of the substrate with rate constants k_{SR} and k_{RS} significantly larger than the rates of cyclization.[40] The equilibrium constant K^{dias} is defined by eq 7.

$$[\mathrm{Ln}] = [\mathrm{cat.}-\mathrm{S}] + [\mathrm{cat.}-\mathrm{R}] \tag{6}$$

$$K^{\mathrm{dias}} = \frac{k_{\mathrm{SR}}}{k_{\mathrm{RS}}} = \frac{[\mathrm{cat.}-\mathrm{R}][\mathrm{S}]}{[\mathrm{cat.}-\mathrm{S}][\mathrm{R}]} \tag{7}$$

The rate of hydroamination/cyclization is first order in catalyst concentration, which corresponds here to the concentration of the substrate/catalyst complexes [cat.−R] and [cat.−S]. Therefore, the rate law for each enantiomer is defined by eqs 8 and 9.[41]

Scheme 5

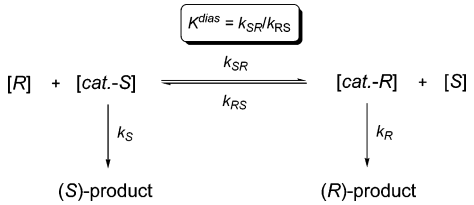

$$-\frac{\mathrm{d[R]}}{\mathrm{d}t} = k_{\mathrm{R}}[\mathrm{cat.}-\mathrm{R}] \tag{8}$$

$$-\frac{\mathrm{d[S]}}{d\mathrm{t}} = k_{\mathrm{S}}[\mathrm{cat.}-\mathrm{S}] \tag{9}$$

Combination of eqs 6−9 and integration[30] leads to

$$f = K^{\mathrm{dias}}\frac{k_{\mathrm{R}}}{k_{\mathrm{S}}} = \frac{\ln([\mathrm{R}]/[\mathrm{R}]_0)}{\ln([\mathrm{S}]/[\mathrm{S}]_0)} \tag{10}$$

The resolution factor can be expressed as a function of conversion *C* and enantiomeric excess ee.

$$f = \frac{\ln[(1-C)(1-\mathrm{ee})]}{\ln[(1-C)(1+\mathrm{ee})]} \tag{11}$$

Note that eq 11 is identical to that obtained for kinetic resolution with a first-order rate dependence in substrate concentration, except that in the latter case the parameter *f* is determined only by the ratio between k_R and k_S.[37a]

Rearrangement of eq 11 leads to an expression for the conversion as a function of the enantiomeric excess ee and the resolution factor *f*, which is in good agreement with the experimental data (Figure 7).

$$C = 1 - \left(\frac{1-\mathrm{ee}}{(1+\mathrm{ee})^f}\right)^{1/(f-1)} \tag{12}$$

Kinetic measurements of the cyclization rates of enantiopure (*S*)-**15e** using either (*R*)-**2**-**Y** or (*S*)-**2**-**Y** provided the rate constants k_{slow} and k_{fast} for the cyclization of the mismatching and matching substrate/catalyst combination (Figure 8).[42] The

(39) Katritzky, A. R.; Cui, X.-L.; Yang, B.; Steel, P. J. *J. Org. Chem.* **1999**, *64*, 1979.

(40) Addition of 10 equiv of *n*-propylamine to (*R*)-**2**-**Y** gave only one broad signal set for the propyl group, while two separate signal sets for the propyl amido group and the coordinated propylamine were observed when only 2 equiv of *n*-propylamine were added. Marks and co-workers observed similar exchange processes with amido amine lanthanocene complexes.[8b]

(41) Note that k_R and k_S are the apparent rate constants for a certain initial substrate concentration. According to the overall rate law in eq 5, they depend on the total base concentration.

(42) In the beginning of the kinetic resolution of *rac*-**15e** with (*R*)-**2**-**Y** (at <50% conversion) the rate of the reaction approaches the zero-order rate of the matching substrate/catalyst combination[41] because, predominantly, the matching substrate enantiomer is consumed. At higher conversions (>60%) most of the matching substrate enantiomer is consumed, and the mismatching substrate enantiomer is consumed with a zero-order rate approaching that of the mismatching substrate/catalyst combination. A smooth transition between these two limiting cases results from the shift of the equilibrium between the two diastereomeric substrate/catalyst complexes (Scheme 5) in favor of the mismatching substrate/catalyst complex during the course of the reaction. The overall time dependence of the concentration of the (*S*) and (*R*) enantiomers during the kinetic resolution process can be expressed by the following equations:[30]

$$[S]_0 - [S] + K^{\mathrm{dias}}\,[R]_0/[S]_0{}^f\;1/f\;([S]_0{}^f - [S]^f) = k_S[Ln]\cdot t$$

$$[R]_0 - [R] + 1/K^{\mathrm{dias}}\,[S]_0/[R]_0{}^{1/f}\;f([R]_0{}^{1/f} - [R]^{1/f}) = k_R[\mathrm{Ln}]\cdot t.$$

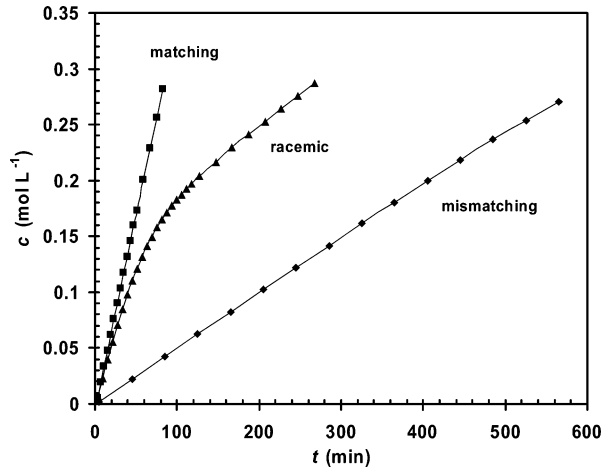

Figure 8. Time dependence of *trans*-product concentration in the cyclization of (*S*)-**15e** using (*S*)-**2-Y** (■) or (*R*)-**2-Y** (◆), as well as in the kinetic resolution of (*rac*)-**15e** using (*R*)-**2-Y** (▲) at 60 °C ([Ln] = 0.0066 mol L^{-1}; $[subst.]_0$ = 0.335 mol L^{-1}).[42]

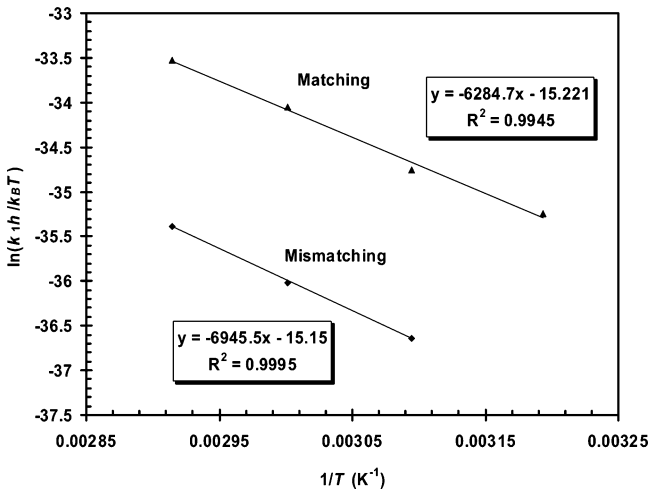

Figure 9. Eyring plot for the hydroamination/cyclization of (*S*)-**15e** using (*S*)-**2-Y** (▲) and (*R*)-**2-Y** (◆).

Eyring plot for k_{fast} and k_{slow} (Figure 9) provided the activation parameters for the matching substrate/catalyst combination ($\Delta H^{\ddagger}$ = 52.2(2.8) kJ mol^{-1}, $\Delta S^{\ddagger} = -127(8)$ J K^{-1} mol^{-1}) and for the mismatching substrate/catalyst combination ($\Delta H^{\ddagger}$ = 57.7-(1.3) kJ mol^{-1}, $\Delta S^{\ddagger} = -126(4)$ J K^{-1} mol^{-1}). The difference in the activation enthalpy is $\Delta\Delta H^{\ddagger}$ = 5.5(3.0) kJ mol^{-1}, while the activation entropy for both transition states is identical within experimental error.

Extrapolation of the Eyring plot gave a relative rate k_{fast}/k_{slow} = 8.2 at 30 °C. Based on the resolution factor f = 14.5 the equilibrium constant of the two substrate/catalyst complexes was estimated to K^{dias} = 1.8, indicating that the equilibrium favors the matching substrate/catalyst diastereomeric complex in this example.

The *trans*/*cis* ratio for the matching substrate/catalyst combination (*S*)-**15e**/(*S*)-**2-Y** was ≥50:1 throughout the reaction, similar to the selectivity observed in the kinetic resolution of racemic **15e** up to 50% conversion.[43] The *trans*/*cis* selectivity of the mismatching substrate/catalyst combination (*S*)-**15e**/(*R*)-**2-Y** on the other hand remained constant at an approximately 13:1 ratio up to 80% conversion, but dropped to an 8.8:1 final ratio (Figure S15).[30]

Discussion

The binaphtholate catalysts **2**−**4** combine high activity and good enantioselectivity. They have catalytic activity similar to highly active lanthanocene catalysts. Cyclization of **5b** with (*R*)-**4a** (94 h^{-1} at 22 °C) proceeded with a turnover frequency identical within margin of error to that of [Cp*$_2$LaCH(SiMe$_3$)$_2$] (95 h^{-1} at 25 °C).[8b] Cyclization of **5a** catalyzed by (*R*)-**4a** (37 h^{-1} at 22 °C) and (*R*)-**2-Y** (2.6 h^{-1} at 25 °C, 93 h^{-1} at 60 °C) should be compared to [Cp*$_2$LaCH(SiMe$_3$)$_2$] (140 h^{-1} at 60 °C),[8b] [(R,S)-neomenthylNdCH(SiMe$_3$)$_2$] (93 h^{-1} at 25 °C),[9b] and [(*R*,*S*)-neomenthylYCH(SiMe$_3$)$_2$] (4 h^{-1} at 25 °C).[9b]

The enantioselectivities observed for catalysts (*R*)-**2-Ln** and (*R*)-**3-Ln** are among the highest reported thus far for rare earth metal based hydroamination catalysts. Livinghouse recently reported the application of an aminothiophenolate catalyst system which gave up to 89% ee,[15f] although catalytic activity was significantly lower than for catalysts **2**−**4**.[44] The two additional amine donors of the amino(thio)phenolate ligands in the catalyst systems reported by Scott[15a] and Livinghouse[15f] seem to reduce catalytic activity, as the metal center becomes less electropositive. Note, however, that one additional amine donor in the ligand, as found in diamidoamine hydroamination catalysts,[14g] does not seem to have a detrimental effect on catalytic activity. The bis-oxazolinato catalyst system reported by Marks was quite catalytically active but failed to give enantioselectivities exceeding 67% ee.[45] Collin, Trifonov, and co-workers reported up to 70% ee using diamidobinaphthylate complexes[15d,g] for the cyclization of the highly activated substrate **5d**.

The apparent zero-order rate dependence on substrate concentration, the first-order rate dependence on catalyst concentration, and the observed activation parameters are in accordance with the generally accepted mechanism for rare earth metal catalyzed hydroamination/cyclizations, in which the insertion of the olefin moiety into the rare earth metal amido bond in a chairlike transition state is the rate-limiting step of the catalytic cycle (Scheme 6).[8b,46] However, the impediment of the reaction at high initial substrate concentrations indicates that a catalytically active binaphtholate amido amine species **A** is in equilibrium with a catalytically inactive or significantly less active binaphtholate amido diamine species **B**.[36a,b] Although lanthanocene catalysts are also slightly inhibited by the presence of external bases, such as *n*-propylamine or THF, they do not show reduced rates with increasing substrate concentration.[8b,34] A significant difference of the binding constants of the aminoalkene starting material and pyrroldine product would result in self-inhibition or self-acceleration due to a shift in the equilibrium of species **A** and **B**.[47] The observation of a zero-order rate

(43) Additionally, cyclization of racemic **15a** with (*R*)-**2-Y** proceeded with 11:1 diastereoselectivity up to 50% conversion, but dropped to 3.4:1 at 100% conversion.

(44) Cyclization of **5b** using 5 mol % of an aminothiophenolate yttrium catalyst required 23 d at 30 °C and 15 h at 60 °C to achieve >95% conversion,[15f] suggesting approximate turnover rates of 0.04 h^{-1}, respectively 1.3 h^{-1}.

(45) Cyclization of **5b** using 5 mol % of a bisoxazolinato lanthanum catalyst proceeded with 67% ee and 25 h^{-1} at 23 °C, whereas **5a** was cyclized in 40% ee with 0.09 h^{-1}.[15c]

(46) (a) Motta, A.; Lanza, G.; Fragalà, I. L.; Marks, T. J. *Organometallics* **2004**, *23*, 4097. (b) Note, however, that in case of the hydroamination/cyclization of aminodienes Tobisch recently proposed turnover-limiting protonolysis of the η^3-butenyl-Ln functionality; see: Tobisch, S. *J. Am. Chem. Soc.* **2005**, *127*, 11979.

Scheme 6

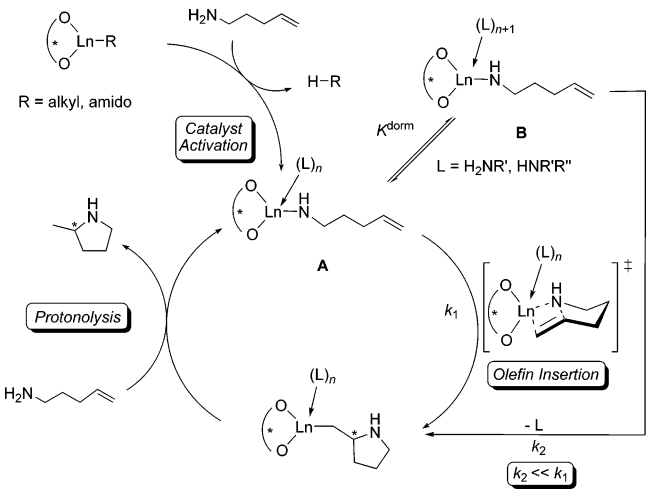

dependence on substrate concentration is therefore indicative of a relative nonspecific binding of the amine bases to the metal center in this example.

The slightly increased catalytic activity of sterically more encumbered 3,3′-bis(tris(3,5-xylyl)silyl)-substituted binaphtholate catalysts (*R*)-**3-Ln** in comparison to that of sterically less demanding 3,3′-bis(triphenylsilyl)-substituted binaphtholate catalysts (*R*)-**2-Ln** can therefore be explained with a weaker binding of amines to (*R*)-**3-Ln**, thereby shifting the equilibrium from the dormant species **B** to the catalytically active species **A**.

Since the equilibrium between species **A** and **B** is shifted at high initial substrate concentrations or in the presence of excess THF, the reaction is channeled more and more through the significantly less active species **B**. The slightly reduced enantioselectivities observed under these conditions could therefore be explained with a less enantioselective cyclization process in species **B**, due to a more crowded coordination environment around the metal center.

The unusual temperature dependence of enantioselectivity in the cyclization of substrate **5b** (Figure S9) is also in agreement with a less selective species **B**, as the equilibrium between species **A** and **B** is shifted at elevated temperatures in favor of the more selective species **A**.

The rate- and stereo-determining olefin insertion step can be proposed to involve an approach of the olefin from the equatorial position to the axial Ln−N bond (Figure 10).[48] The transition state for an approach of the Ln−N bond to the *si* face of the olefin, leading to the (*R*)-pyrrolidine product, is hampered by sterically unfavorable interactions of the substrate with one of the sterically demanding tris(aryl)silyl substituents, whereas no

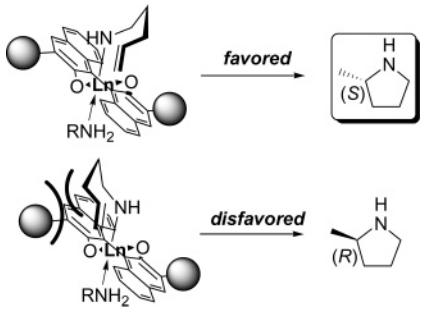

Figure 10. Stereomodel for enantioselective hydroamination/cyclization of aminoalkene **5a** by binaphtholate rare earth metal catalysts with an equatorial approach of the olefin.

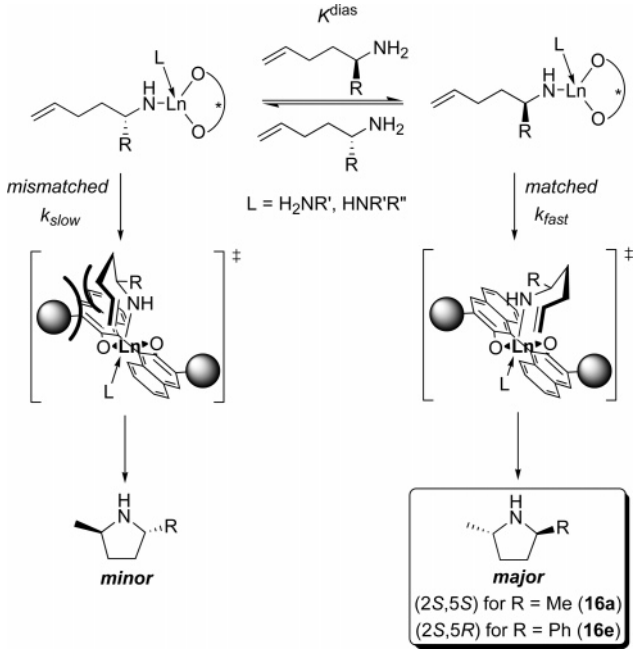

Figure 11. Proposed stereochemical model for the kinetic resolution of α−substituted 1-aminopent-4-enes.

such interaction occurs if the olefin approaches with the opposite *re* face to give the observed (*S*) stereochemistry. The effect of different bases coordinated to species **A** (either aminoalkene substrate, pyrrolidine product, or THF) can be expected to have only a minimal influence on the stereoselection process, as the exogenous base coordinates *trans* to the axial Ln−N bond, which is also in accordance with conversion-independent product enantioselectivities.

In agreement with these observations, the cyclization of chiral aminoalkenes **15a**−**g** proceeded also preferentially through an approach of the Ln−N bond to the *re* face of the olefin. In case of the matching substrate/catalyst combination the α-substituent preferentially rests in an equatorial position, locking the conformation of the seven-membered cyclization transition state, and allowing a facile approach of the Ln−N bond to the *re* face of the olefin (Figure 11). In case of the mismatching substrate/catalyst combination the approach to the *si* face of the olefin with an equatorial α-substituent is hindered by sterically unfavorable interactions between the substrate and the tris(aryl)silyl substituent. An approach to the *re* face of the olefin on the other hand, favored by diminished steric interactions with the tris(aryl)silyl substituents of the binaphtholate ligand, requires an α-substituent in axial position and leads to the *cis*

(47) (a) As noted above, the cyclization of **5a** by (*R*)-**2-Y** performed at 25 °C showed a slight sign of curvature (acceleration, see Figures 6 and S5), suggesting that the binding constant of the pyrrolidine product is slightly smaller than that of the aminoalkene. (b) Sterically open *ansa*-lanthanocene complexes and constrained geometry catalysts display product inhibition (apparent first-order kinetics),[8b,9b,d,e] while self-acceleration has been observed in the cyclization of aminodiene derivatives using sterically more encumbered catalysts.[9d] (c) For product inhibition in rare earth metal catalyzed hydrophosphination, see: Douglass, M. R.; Stern, C. L.; Marks, T. J. *J. Am. Chem. Soc.* **2001**, *123*, 10221.

(48) A similar model has been proposed by Marks and co-workers for their bisoxazolinato rare earth metal hydroamination catalyst system.[15c] Molecular modeling studies indicated that the opposite (minor) pyrrolidine enantiomer should form if the olefin approaches from the apical position to an equatorial Ln−N bond. A change of the approach of the olefin was suggested to be responsible for the reversal of product absolute configuration when catalysts with alkyl-substituted bisoxazolinato ligands were used instead of catalysts with aryl-substituted bisoxazolinato ligands.

pyrrolidine product. This competition between enantiomorphic site control and substrate control explains the lower *trans*/*cis* diastereoselectivity observed in the cyclization of the mismatching aminoalkene/catalyst combination (*S*)-**15e** and (*R*)-**2-Y**.

The kinetic resolution process of substrate **15e** is assisted by the equilibrium between the two diastereomeric substrate/catalyst complexes, which lies in favor of the matching substrate/catalyst combination. The low efficiency in the kinetic resolution of alkyl-substituted aminoalkenes **15b**−**d** on the other hand could result from a less favorable position of the substrate/catalyst complexation equilibrium (e.g., $K^{dias} \leq 1$).[49]

A plausible explanation for the high *trans*/*cis* ratio and high efficiency in the kinetic resolution of aryl-substituted substrates **15e**−**15g** in comparison to that of alkyl-substituted substrates **15b**−**15d** could stem from a π-interaction of the aryl substituent with the metal center or one of the aromatic substituents of the binaphtholate ligand. Further evidence for this proposal is indicated by the increased rate of cyclization and improved resolution efficiency in the presence of the electron-donating *p*-methoxy group in **15g**, in comparison to the electron-withdrawing *p*-chloro-substituted **15f**.[50] Similar aryl-directing effects have been shown to be crucial for high regioselectivity in intermolecular vinylarene hydroamination and ring opening of unsymmetrical phenylmethylenecyclopropanes.[10b]

Conclusion

Rare earth metal complexes with sterically demanding tris(aryl)silyl-substituted binaphtholate ligands are efficient catalysts for asymmetric hydroamination/cyclization of aminoalkenes and the kinetic resolution of α-substituted aminopentenes. Catalytic activities are comparable to those of lanthanocene catalyst systems, and enantioselectivities of up to 95% ee were achieved in the cyclization of achiral aminopentenes. The hydroamination mechanism for the binaphtholate catalyst system is similar to that proposed for lanthanocene catalysts, based on the rate dependencies on substrate and catalyst concentrations and the observed activation parameters. However, the binaphtholate complexes are more prone to base coordination, as exemplified by the dependence of catalytic activity on initial substrate concentration. Further studies will focus on the scope, selectivity, and functional group tolerance of the binaphtholate rare earth metal complexes in asymmetric hydroamination and other catalytic σ-bond metathesis reactions. The initial experiments of the *anti*-Markovnikov addition of *n*-propylamine to styrene indicate that the highly active lanthanum catalysts (*R*)-**4a** and (*R*)-**4b** are the most promising candidates for asymmetric intermolecular hydroamination reactions.

Acknowledgment. Generous financial support by the Deutsche Forschungsgemeinschaft (DFG), the Fonds der Chemischen Industrie, and the Dr. Otto Röhm Gedächtnisstiftung is gratefully acknowledged. K.C.H. is a DFG Emmy Noether fellow (2001−2006) and thanks Professor John A. Gladysz for his continual support. We thank Patricia Horrillo Martínez for the preparation of substrates **5c** and **5d**, Rebekka Park for assistance in the preparation of substrates **15f** and **15g** and some kinetic resolution experiments, as well as Dmitri Denysenko for helpful discussions.

Supporting Information Available: Experimental procedures and spectral and analytical data for complexes, substrates and products, derivation of equations, kinetic diagrams, and crystallographic data (in CIF format) for (2*R*,5*S*)-**16e**·HCl and the Mosher amide of (*S*)-**6c**. This material is available free of charge via the Internet at http://pubs.acs.org.

JA058287T

(49) Further kinetic studies will address this subject.
(50) The fact that the *p*-methoxy functionality in substrate **15g** is tolerated by (*R*)-**2-Y** without detrimental effect on the rate of cyclization can be explained by the remote position of the methoxy substituent.